IJISET - International Journal of Innovative Science, Engineering & Technology, Vol. 1 Issue 2, April 2014.
www.ijiset.com
ISSN 2348 - 7968

Design and simulation of Two Dimensional Photonic Crystal Ring Resonator based Four Port Wavelength Demultiplexer

T. Saraniya[1], S. Robinson[2], and K. Vijaya Shanthi[3]

[1]PG Scholar, Communication Systems, Mount Zion College of Engineering and Technology, Pudukkottai-622507,Tamil Nadu, India

[2]Associate Professor, Department of Electronics and Communication Engineering, Mount Zion College of Engineering and Technology, Pudukkottai-622507, Tamil Nadu, India

[3]PG Scholar, Communication Systems, Mount Zion College of Engineering and Technology, Pudukkottai-622507,Tamil Nadu, India

Abstract

In this paper, a four port wavelength demultiplexer based on two dimensional Photonic Crystal ring resonator is designed. By varying the index differences of 2.43, 2.46 and 2.49 for each port, the dropping and the coupling efficiencies are obtained. The results of simulation is done by Finite Difference Time Domain method, which is highly suitable for Photonic Integrated Circuits. By varying the index differences, various wavelengths can be obtained, so the device is tunable.

Keywords: *Photonic crystal ring resonator, photonic band gap, Demultiplexer, FDTD method, PWE method*

1. Introduction

In earliest technology, devices that can be designed in the range of centimeter and millimeter. Photonic Crystal (PC) based technology attracted the researchers which can be implemented in nanometer. The most prominent and recent technology of designing the Demultiplexer (DEMUX) is using of Photonic Crystals. Photonic Crystals are composed of periodic dielectric or nanostructures that affect the propagation of electromagnetic waves (EM) [1] and contain regularly repeating regions of high and low dielectric constant. Wavelengths that are allowed to travel are known as modes; groups of allowed modes form bands. Disallowed bands of wavelengths are called as Photonic Band Gaps (PBGs). The light cannot propagate in the PBG region i.e. there are no modes and no spontaneous emission in this region [1]. By introducing point and line defect in these structures, the periodicity and thus the completeness of the band gap are disturbed and the propagation of light can be localized in the PBG region. Generally, Photonic Crystal (PC) based optical devices have attracted great interest due to their compactness, speed of operation, long life and suitability for Photonic Integrated Circuits (PIC). One of the most promising designs for DEMUX is ring resonator. Generally, ring resonators have received great attention in research community, as it offers high spectral selectivity, scalability, narrow channel spacing, efficient wavelength selection, and wide free spectral range.

Demultiplexer (DEMUX) [9] is one of the most significant device that is used to separate signals from the multiplexed output channels. This device separates one signal in to several streams of signals and are often used in telecommunications to carry signals over long distances. However, design of PCs based devices would result the dimension of the devices in the order of micrometers.

In the literature, the square lattice based DEMUX is done by introducing point defects and/or line defects [17] and using PCRR [19].

In this paper, a four port circular PCRR [19] based DEMUX is proposed by varying the index differences for each port using two dimensional (2D) PCs is designed. The PWE method is the most popular method to calculate the band gaps of the structure which is used for calculating the PBG with and without introducing any defects. The normalized transmission spectra and the resonant wavelength is calculated by FDTD method.

The paper is arranged as follows: In Section 2, the numerical analysis method namely FDTD and PWE are discussed. The PBG of structure with and without introducing defects and also the design of DEMUX is explained in Section 3 and 4. The simulation results of proposed DEMUX is discussed in Section 5 and the Section 6 concludes the paper.

2. Numerical Analysis

Inorder to analyze the dispersion behavior and the transmission spectra of PCs, PWE [37] and FDTD [36] methods are used. The PWE method is useful for analyzing the PC structures, that can be expressed as a superposition of a set of plane waves [37]. Although this method can obtain an accurate solution for the dispersion properties (propagation modes and band gap) of a PC structure. An alternative approach which has been widely adopted to calculate both transmission spectra and field distribution is based on numerical solutions of Maxwell's equations by using FDTD method [36]. In this analysis, the PWE is used to calculate the band gap and propagation modes of the PC structure, whereas 2D FDTD is used to calculate the spectrum of the power transmission.

The Maxwell's Equations are useful for analyzing the propagation of electromagnetic waves in a photonic crystal. It is assumed that the material is linear, isotropic, periodic with lattice vector and lossless; therefore, the Maxwell's equations have the following form [36].

$$\frac{\partial H}{\partial t} = -\frac{1}{\mu}\nabla \times E \qquad (1)$$

$$\frac{\partial E}{\partial t} = \frac{1}{\varepsilon}\nabla \times H \qquad (2)$$

where '*E*' and '*H*' are the electric and magnetic fields, and 'ε' and 'μ' are the dielectric constant and permeability.

2.1 PWE Method

The band diagram [37] is the most common representation of the band structure of PCs which gives the propagation modes and PBG. The PBG is the main characteristics of photonic devices and can be observed using the band diagrams obtained through the PWE method. It is employed both for electric and magnetic fields and the periodic dielectric structure is expanded in Fourier series. This output can be represented as the region within the boundary of irreducible Brillouin zone. In this, X-axis is divided into regions representing the line segments connecting the Γ−X−M−Γ points in wave vector space and Z-axis is the normalized frequency (ωa/2Πc=a/λ) of electromagnetic waves that propagate in the photonic crystal.

The band diagram calculations of electric field are carried out by solving Maxwell's equation which is

$$\nabla \times \left(\frac{1}{\varepsilon(r)} \nabla \times E(r) \right) = \frac{\omega^2}{c^2} E(r) \qquad (3)$$

where '*c*' is the speed of light, 'ω' is the angular frequency, $\varepsilon(r)$ is the dielectric constant (relative permittivity) and $E(r)$ is the electric field of the periodic function.

The above equation describes the propagation of light in photonic crystals and it is a consequence of the Bloch-Floquet theorem which signifies that the electromagnetic waves in the periodic media can propagate without scattering and their behavior governed by a periodic function modulated by a plane wave (the product of plane wave and periodic function with lattice period).

Because of the periodic 2D PC, the dielectric constant, ε can be described as

$$\varepsilon(r) = \varepsilon(r + R) \qquad (4)$$

where R is the vector of the 2D lattice.

Bolch-Floquet theorem provides the solutions for periodic eigen problem that can take the form

$$H_k(r) = e^{ikr} u_k(r) \qquad (5)$$

where $u_k(r)$ is the periodic function of lattice that is

$$(i\mathrm{k}+\nabla)\times\frac{1}{\varepsilon(r)}(i\mathrm{k}+\nabla)\times u_{\mathrm{k}}(r) = \frac{\omega(\mathrm{k})^2}{c^2} u_{\mathrm{k}}(r) \qquad (6)$$

For a given choice of Bloch vector *k*, the eigen value Eq.(5) is discretized into a plane wave basis to yield an algebraic eigen value problem. It is solved for the permissible frequencies ω of the modes, which, in turn, are characterized by the eigen vectors. By scanning *k* over the Brillouin zone, the band diagram is generated.

2.2 FDTD Analysis

$$E_x\Big|_{i,j}^{n+1} = E_x\Big|_{i,j}^{n} + \frac{c\Delta t}{\varepsilon_0}\left[\frac{H_z\Big|_{i,j+1/2}^{n+1/2} - H_z\Big|_{i,j-1/2}^{n+1/2}}{\Delta y}\right] \qquad (7)$$

$$E_y\Big|_{i,j}^{n+1} = E_y\Big|_{i,j}^{n} - \frac{c\Delta t}{\varepsilon_0}\left[\frac{H_z\Big|_{i+1/2,j}^{n+1/2} - H_z\Big|_{i-1/2,j}^{n+1/2}}{\Delta x}\right] \qquad (8)$$

$$H_z\Big|_{i,j}^{n+1/2} = E_z\Big|_{i,j}^{n-1/2} + \frac{c\Delta t}{\mu_0}\left[\left(\frac{E_x\Big|_{i,j+1/2}^{n} - E_x\Big|_{i,j-1/2}^{n}}{\Delta y}\right) - \left(\frac{E_y\Big|_{i+1/2,j}^{n} - E_y\Big|_{i+1/2,j}^{n}}{\Delta x}\right)\right] \qquad (9)$$

where the index 'n' denotes the discrete time step, indices 'i' and 'j' denote the discretized grid point in the X-Y plane. These equations [36] are iteratively solved in a leap frog manner, alternating between computing the E and H fields at subsequent Δt/2 intervals.

In order to produce an accurate simulation, the spatial grid must be small enough to resolve the smallest feature of the field to be simulated. To obtain a stable simulation, one must satisfies the following condition which relates the spatial and temporal step size.

$$\Delta t \le \frac{1}{c\sqrt{\frac{1}{\Delta x^2}+\frac{1}{\Delta y^2}}} \qquad (10)$$

where 'c' is the speed of the light.

A broadband Gaussian pulse is launched into input port. Then we place a time monitor (detector) inside each waveguide channel to measure the time varying electric field. The time monitor is used to record the power flow along the Z direction as the function of time. The output power is calculated at each port by integrating the power over the cells of the output ports as shown in Eq.(9). Then the stored data is Fourier transformed and integrated. Finally, the ratio is taken between obtained integrated results to incident spectra which results in transmission spectra versus wavelength. The output signal power is

$$P(t) = \frac{\mathrm{Re}\left[\int_A [E(t)\times H^*(t)]\,dA\right]}{\mathrm{Re}\left[\int_A [E(t_0)\times H^*(t_0)]\,dA\right]} \qquad (11)$$

where 'E' and 'H' are the electric and magnetic fields, and 'A' is the plane located within the domain of the time monitor. The length of the time monitor has no effect for a power as the integral is taken over the plane defined by the X' and Z` axis.

3. Structure Design

The perfect lattice of proposed four port wavelength DEMUX consists of square array of circular rods placed in a background of air. The number of rods in 'X' and 'Z' directions are 49 and 21. The distance between two adjacent rods are 590nm which is termed as lattice constant and denoted by 'a'. The radius of the rod is 0.1μm and the index differences that have been used in second, third and the fourth PCRRs are 2.43, 2.46 and 2.49. The band diagram [37] in **Fig.1** gives the propagation modes of the structure without defect whose corresponding Brillouin zone is also shown in **Fig.2.**

The Brillouin zone is the smallest repeating space in the periodic structure; hence the band diagram of single zone is equal to the whole zone. The band diagram shown in **Fig.1** has PBG for Transverse Electric (TE) modes whose electric field is parallel to the rod axis. The PC structure has a PBG for TE ranges from 0.32 a/λ to 0.44 a/λ whose corresponding wavelength accounts from 1340 nm to 1843nm.The frequency of the PC structure is $\omega a/2\Pi c = a/\lambda$, where 'ω' is the angular frequency, '*a*' is the lattice constant, '*c*' is the velocity of light in free space and 'λ' is the free space wavelength.

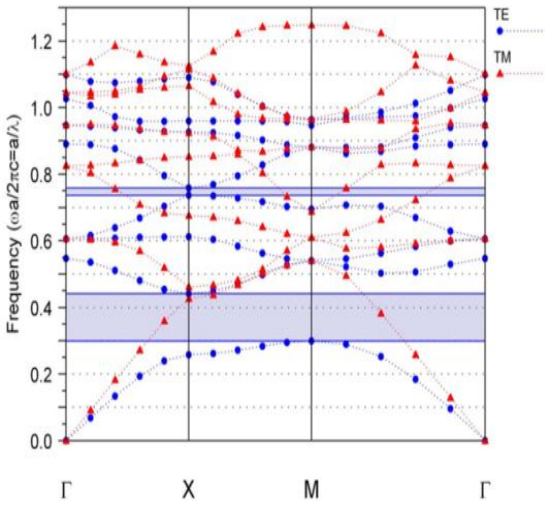

Fig. 1 Band diagram of 1*1 PC square lattice structure.

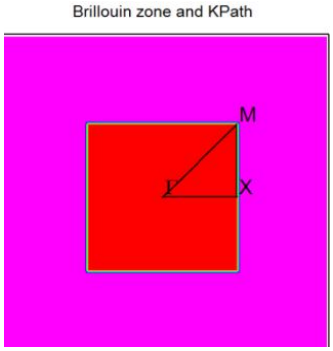

Fig. 2 Brillouin zone and kpath of 49*21 PC structure.

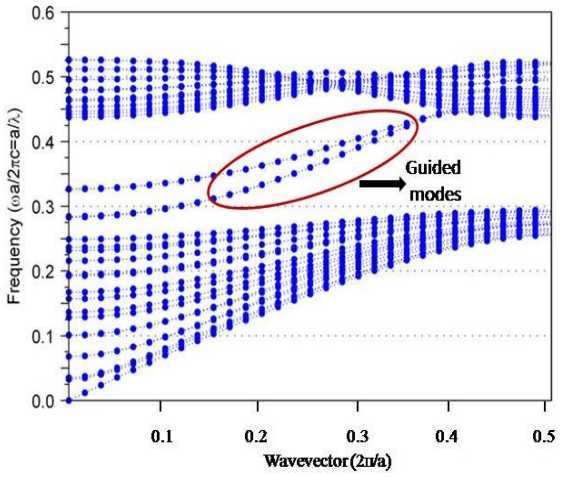

Fig. 3 Band diagram of 49*21 PC structure after the introduction of line and point defects.

When the defects (line and point) are created in the structure, the completeness of the PBG is broken and the guided modes (even and odd modes) are propagated inside PBG region as shown in **Fig. 3.** It shows there are two modes (even and odd) propagate inside the PBG region which is essential for complete signal transfer from the bus waveguide to drop waveguide through ring resonator at resonance.

4. Photonic Crystal Ring Resonator

In general, the resonators [28] are located between two optical waveguides. The proposed structure consists of four ports one is to transfer the power from input port 'A' to the output port 1 'B' and the other at the resonating output ports 2'C', 3'D' and 4'E'. The **Fig. 4** sketch the four port circular PCRR based DEMUX which consists of one optical waveguide in horizontal (r-x) direction and a three circular PCRR below the optical waveguide. The first PCRR is having the index difference of 2.43, the second one is having 2.46 and the third one has 2.49. The top waveguide is called as bus waveguide whereas the bottom waveguides are known as dropping waveguides. The bus waveguide is formed by introducing line defects whereas the circular PCRR is shaped by point defects (i.e. by removing the column rods to make a circular shape). The circular PCRR is formed by varying the position of inner rods and outer rods from their original position towards center of the origin. To avoid the backward propagation, the scatterer rods are placed at each corner of the four sides inorder to enhance the coupling efficiency.

The input signal port is marked as 'A' with arrow in the left side of bus waveguide, while the 'B' of the right side of bus waveguide is defined as the forward transmission terminal, while the 'C','D' and 'E' are defined as the resonating outputs. The power is travelling in the bus waveguide and the wavelength exits to the output port 1 'B'. At one resonance, the wavelength is coupled into the ring resonator [22] from bus waveguide and dropping the suitable wavelength to the output ports, 2 'C', 3 'D' and 4 'E'. The coupling and dropping efficiencies are detected by monitoring the power at ports , 'B','C', 'D' and 'E', respectively

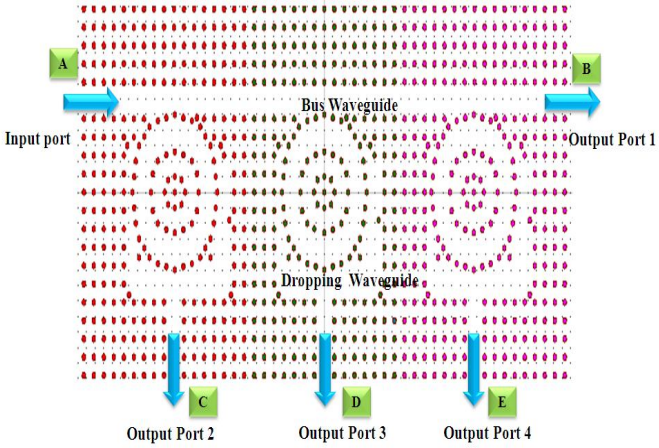

Fig. 4 Schematic structure of 2D four port circular PCRR based DEMUX.

5. Simulation Results

A Gaussian input signal [3] is launched into the input port 'A'. The normalized transmission spectra at ports 'B','C', 'D' and 'E' is obtained by conducting the Fast Fourier Transform (FFT) [36] of the fields that are calculated by 2D-FDTD method. The output signal powers are recorded through power monitors by placing them at appropriate ports. The normalized transmission is calculated through the following formula:

$$T(f) = \frac{1/2\int real(p(f)^{monitor}).dS}{SourcePower} \quad (12)$$

Where T(f) is normalized transmission which is a function of frequency, p(f) is poynting vector and dS is the surface normal.

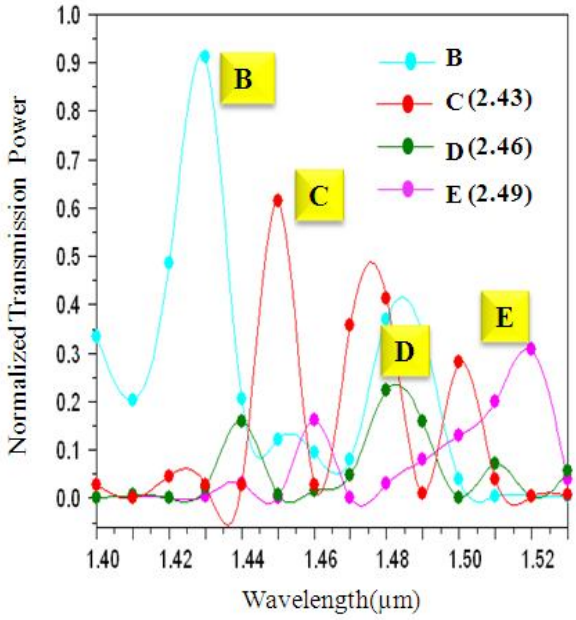

Fig. 5 Normalized transmission spectra of four port circular PCRR based DEMUX.

Fig. 5 shows the normalized transmission spectra of DEMUX. By varying the index differences of 2.43, 2.46 and 2.49 for each port, the OFF resonance wavelength of the proposed DEMUX is observed at 1430nm and the ON resonance wavelengths are 1450nm, 1480nm and 1520nm. The obtained results are efficiently suitable for demultiplexing applications. The quality factor and the transmission power efficiencies are tabulated as shown in **Table. 1.**

Table. 1 Simulation results of four port wavelength division demultiplexer

Output Port	λ0(nm)	Q	Transmission
1 (B)	1430	71.5	91%
2 (C)	1450	111.5	61.5%
3 (D)	1480	148	22%
4 (E)	1520	152	30%

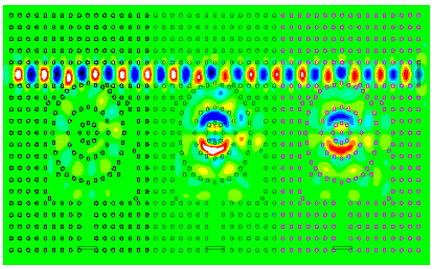

(a)

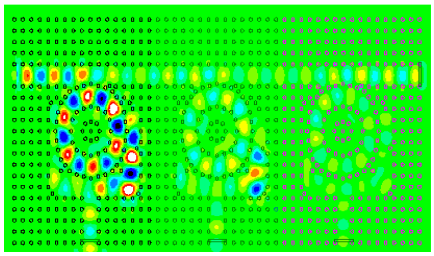

(b)

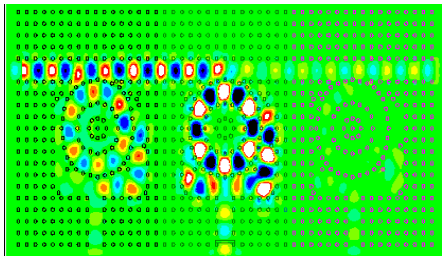

(c)

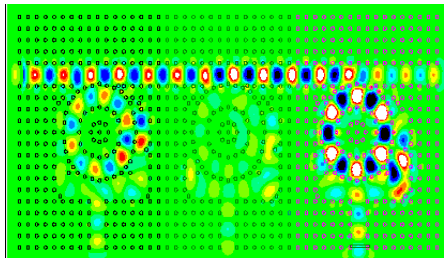

(d)

Fig. 6 Electric field pattern of four port circular PCRR based DEMUX (a). OFF resonance at 1430nm (b). ON resonance for the index difference 2.43 at 1450nm (c). ON resonance for the index difference 2.46 at 1480nm and (d). ON resonance for the index difference 2.49 at 1520nm.

The **Figs. 6** depict the electric field pattern of four port circular PCRR based DEMUX. The **Fig. 6. (a)** denote the OFF resonance wavelength at 1430nm. The **Figs. 6. (b), (c)** and **(d)** denote the ON resonance wavelength for the index differences of 2.43, 2.46 and 2.49 are 1450 nm, 1480nm and 1520nm, respectively. At resonant wavelength, λ=1450 nm, 1480 nm and 1520nm, the electric field of the bus waveguide is fully coupled into the ring resonator and reached the output ports 'C', 'D' and 'E', whereas at off resonance λ=1430nm, the signal directly reaches the forward transmission terminal. The quality factor (Q) that characterizes the resolution of wavelength selecting and can be calculated as $Q=\lambda 0/\Delta\lambda$ (where λ0 and Δλ are central wavelength and full width at half power of output and bandwidth, respectively.

6. Conclusions

A design and analysis of four port wavelength demultiplexer based on two dimensional Photonic Crystal ring resonator had been introduced and investigated through 2D FDTD method. By varying the index differences of 2.43, 2.46 and 2.49 for each port, the desired wavelength of output power can be obtained. It means that the output wavelengths are easily tunable. The coupling and the dropping efficiencies are obtained by means of simulation. Hence, such kinds of devices would be more useful to Photonic Integrated Circuits and realization of WDM systems for future optical networks.

References

[1] E. Yablonovitch, "Inhibited spontaneous emission on solid-state physics and electronics", Phys. Rev. Lett, Vol. 58, No. 20, 1987, pp. 2059-2062.
[2] S. John, "Strong localization of photons in certain disordered dielectric superlattices", Phys. Rev. Lett, Vol. 58, No. 23, 1987, pp. 2486-2489.
[3] J. D. Joannopoulos, R. D. Meade, and J. N. Winn, "photonic crystal: Modeling of flow of light", Princeton, NJ: Princeton university press, 1995.
[4] J. D. Joannopoulos, P. R. Villeneuve and S. Fan, "Photonic crystals: putting a new twist of light", Nature, 1997,Vol. 386, pp. 143-149.
[5] Dan Sadot and Efraim Boimovich, "Tunable optical filters for dense WDM networks", IEEE Communications Magazine, 1998, pp. 50-55.
[6] S. Riaz Ahemed, "Performance Analysis of DWDM", Journal of Theoretical and Applied Information Technology, 2005, pp. 590-594.
[7] A. Ghaffari, F. Monifi, M. Djavid, and M. S. Abrishamian, "Analysis of photonic crystal power splitters with different configurations", Journal of Applied Science, Vol. 8, 2008, pp. 1416-1425.
[8] G. Manzacca, D. Paciotti, A. Marchese, M. S. Moreolo, G. Cincotti, "2D photonic crystal cavity-based WDM multiplexer", Photonics and Nanostructures-Fundamentals and Applications, Vol. 5, 2007, pp. 164-170.
[9] A. Ghaffari, F. Monifi, M. Djavid, and M. S. Abrishamian, "Heterostructure wavelength division demultiplexers using photonic crystal ring resonators", Optics Communications, Vol. 281, 2008, pp. 4028-4032.
[10] V. Zabelin, L. A. Dunbar, N. Le Thomas, R. Houdre, M. V. Kotlyar, L. O. Faolain and T.F. Krauss, "Self-collimating photonic crystal polarization beam splitter", Opti. Lett, Vol. 32, No.5, 2007, pp. 530-532.
[11] Tien-Tsorng shih, Yaw-Dong Wu, and Jian-Jang Lee, "Proposal for compact optical triplexer filter using 2-D Photonic crystals", IEEE Pho. Tech. Lett, Vol. 21, No. 1, 2009, pp. 18-21.
[12] Qiong Wang, Yiping Cui, Hiayu Zhang, Changchun Yan, Lingling Zhang, "The position independence of heterostructure coupled waveguides in photonic-crystal switch", Optik Optics, Vol. 121, 2010, pp. 684-688.
[13] M. K. Moghaddam, A. R. Attari, M. M. Mirsalehi, "Improved photonic crystal directional coupler with short length", Photonics and Nanostructures-Fundamentals and Applications, Vol.8, 2010, pp. 47-53.
[14] F. Monifi, M. Djavid, A. Ghaffari, and M. S. Abrishamian, "A new bandstop filter based on photonic crystals", Proc. PIER, 2008, pp. 674-677.
[15] M. Djavid, A. Ghaffari, F. Monifi and M. S. Abrishamian, "Photonic crystal narrow band filters using biperiodic structures", Journal of Applied Science, Vol. 8, No.10, 2008, pp. 1891-1897.
[16] S. Robinson, and R. Nakkeeran "A Bandpass Filter Based on 2D Circular Photonic Crystal Ring Resonator", 7th IEEE International Conference on WOCN'10,Sep 6-8, 2010, Colombo, Sri Lanka.
[17] S. Fan, P. R. Villeneuve, J. D. Joannopoulos, H. A. Haus "Channel drop filters in photonic crystals", Opti. Express, Vol. 3, No. 1, 1998, pp. 4-11.
[18] Chun- Chih Wang, Lien-Wen Chen, "Channel drop filters with folded directional couplers in two-dimensional photonic crystals", Physica B, Vol. 405, 2010, pp. 1210-1215.
[19] S. Robinson, and R. Nakkeeran "Channel Drop Filter based on 2D Square-Lattice Photonic Crystal Ring Resonator", 7th IEEE International Conference on WOCN'10, Sep 6-8, 2010, Colombo, Sri Lanka.
[20] Min Qiu and Bozepa Jaskorzynska, "Design of a channel drop filter in a two-dimensional triangular photonic crystal", Applied Physics Letters, Vol. 83, No. 6, 2003, pp. 1074 -1076.
[21] Hongliang Ren, Chun Jiang, Weisheng Hu, Mingyi Gao, Yang Qu, and Fanghua Wang, "Channel drop filter in two-dimensional triangular lattice photonic crystals," Opti. Express, Vol. 24, No. 10, 2007, pp. A7-A11.
[22] M. David, A. Ghaffari, F. Monifi, M. S. Abrishamian, "T-Shaped channel drop filters using photonic crystal ring resonators",,Physica E, Vol. 40, 2008, pp. 3151-3154.
[23] B. S. Darki, N. Granpayesh, "Improving the performance of a photonic crystal ring-resonator-based channel drop filter using particle swarm optimization method", Optics Communications, in press, Vol. 15232, 2010, pp. 1-5.
[24] J. RomeroVivas1, D. N. Chigrin, A. V. Lavrinenko, and C.M. Sotomayor Torres, "Resonant add-drop filter based on a photonic quasicrystal", Opti. Express, Vol. 13, No. 3, 2005, pp. 826-835.
[25] Z. Qiang, W. Zhou, and Richard A. Soref, "Optical add-drop filters based on photonic crystal ring resonators", Opti. Express, Vol. 15, No. 4, 2007, pp. 1823-1831.
[26] Juan Jose Vegas Olmos, Masatoshi Tokushima, and Kenichi Kitayam, "Photonic add–drop filter based on integrated photonic crystal structures", Journal of Selected Topics in Quantum Electronics, Vol. 16, No. 1, 2010, pp. 332-337.
[27] M. Djavid, A. Ghaffari, F. Monifi, M.S. Abrishamian, "A new broadband photonic crystal add drop filter," Journal of Applied Sciences, Vol.8, No. 11, 2008, pp. 2178-2182.

[28] S. Robinson, and R. Nakkeeran, "Photonic Crystal Ring Resonator Based Add-Drop Filter Using Hexagonal Rods for CWDM Systems", Optoelectronics Letters, Vol. 7, No. 3, 2011, pp. 164-166.
[29] S. Robinson, and R. Nakkeeran, "PCRR based Add drop filter for ITU.G.694.2 CWDM Systems", Optik Optics, Vol. 124, No. 5, 2013, pp. 393-398.
[30] S. Robinson, and R. Nakkeeran, "Two dimensional Photonic Crystal Ring Resonator based Add Drop Filter for CWDM systems", Optik Optics, Vol. 124, No. 6, 2013, pp. 3430-3435.
[31] S. Robinson, and R. Nakkeeran, "Coupled Mode Theory analysis for Photonic Crystal Ring Resonator based Add Drop Filter", Optical Engineering, Vol. 51, No.11, 2012, pp. 1114001-7.
[32] S. Robinson and R. Nakkeeran, "Two Dimensional Photonic Crystal Ring Resonator Based Bandpass Filter for C-Band of CWDM Applications", IEEE NCC 2011, Jan 28-30, 2011, pp. 1-4.
[33] S. Robinson, and R. Nakkeeran, "Investigation on parameters affecting the performance of the two dimensional photonic crystal based bandpass filter", Optical and Quantum Electronics, Vol. 43, No. 6, 2012, pp. 69-82.
[34] S. Robinson, and R. Nakkeeran, "Investigation on Two Dimensional Photonic Crystal Resonant Cavity based Bandpass Filter", Optik Optics, Vol. 123, No. 5, 2012, pp. 451-457.
[35] J. B. Pendry and A. MacKinnon, "Calculation of photon dispersion relation", Phys. Rev. Lett, Vol. 69, 1992, pp. 2772-2775.
[36] A. Taflove, "Computational Electrodynamics", The Finite- Difference Time- Domain Method, Artech House, Boston, London, 2005.
[37] J. B. Pendry, "Calculating photonic band structure", Journal of Phys. Cond. Mat, Vol. 8, 1996, pp.1085-1108.
[38] G. Pelosi, R. Coccioli and S. Selleri, "Quick Finite Elements for Electromagnetic waves" Artech House, Boston, London, 1997.